Journal of Power Sources 254 (2014) 55–61

Contents lists available at ScienceDirect

Journal of Power Sources

journal homepage: www.elsevier.com/locate/jpowsour

Low surface area graphene/cellulose composite as a host matrix for lithium sulphur batteries

Manu U.M. Patel [a], Nguyen Dang Luong [b], Jukka Seppälä [b], Elena Tchernychova [a], Robert Dominko [a,*]

[a] National Institute of Chemistry, Hajdrihova 19, SI-1000 Ljubljana, Slovenia
[b] Laboratory of Polymer Technology, Department of Biotechnology and Chemical Technology, Aalto University, School of Chemical Technology, P.O. Box 16100, FI-00076 Aalto, Finland

HIGHLIGHTS

- Low surface area graphene/cellulose composite as a host matrix for Li-S batteries.
- Graphene serves as electron conductive additive and cellulose as a spacer.
- Cellulose–graphene ratio 1:1 showed the best electrochemical performance.
- Composite enables accommodation of expansion due to formation of Li_2S.

ARTICLE INFO

Article history:
Received 9 October 2013
Received in revised form
29 November 2013
Accepted 17 December 2013
Available online 26 December 2013

Keywords:
Li-S battery
Graphene
Cellulose
Composite
Cycling stability
Coulombic efficiency

ABSTRACT

Graphene/cellulose composites were prepared and studied as potential host matrixes for sulphur impregnation and use in Li-S batteries. We demonstrate that with the proper design of a relatively low surface area graphene/cellulose composite, a high electrochemical performance along with good cyclability can be achieved. Graphene cellulose composites are built from two constituents: a two-dimensional electronic conductive graphene and cellulose fibres as a structural frame; together they form a laminar type of pore. The graphene sheets that uniformly anchor sulphur molecules provide confinement ability for polysulphides, sufficient space to accommodate sulphur volumetric expansion, a large contact area with the sulphur and a short transport pathway for both electrons and lithium ions. Nano-cellulose prevents the opening of graphene sheets due to the volume expansion caused by dissolved polysulphides during battery operation. This, in turn, prevents the diffusion of lithium polysulphides into the electrolyte, enabling a long cycle life.

1. Introduction

Recently, there has been a steady increase in demand for clean, efficient and safe energy due to the increasing diversity of energy applications. One of the important solutions found to meet the energy demand was lithium ion battery system. Due to their high energy density, rechargeable lithium ion batteries have become the dominant power source for portable electronics. Their energy density is limited by cell chemistry, and they do not completely meet the requirements on the field of electromobility [1].

Lithium sulphur (Li-S) batteries are one of the most promising energy conversion alternatives that can meet the demands for the suitable driving range of battery electric vehicles (BEVs). A Li-S battery system has a theoretical capacity of 1675 mAh g^{-1} and an energy density of 2500 Wh kg^{-1}. The abundance of sulphur in nature makes it a cheap raw material, which also reduces the cost of Li-S battery systems [2–5]. However, there are several problems or challenges that have to be solved or addressed in order to reach the expected goal of obtaining a high performance, safe, long life, eco-friendly and inexpensive Li-S battery. As the Li-S system is plagued by the problems of the low electrical conductivity of sulphur, the dissolution and diffusion of polysulphides into the electrolyte, and the volume expansion of sulphur intermediates during battery operation. These problems result in poor life cycle, low specific capacity, and low energy efficiency [6,7]. Recently, a great deal of effort has been made to find a suitable host matrix for sulphur impregnation, which would enhance electrochemical reaction and render polysulphide diffusion [8,9]. Different types of carbon/

* Corresponding author. Tel.: +386 14760362; fax: +38614760300.
E-mail address: Robert.Dominko@ki.si (R. Dominko).

0378-7753/$ – see front matter © 2013 Elsevier B.V. All rights reserved.
http://dx.doi.org/10.1016/j.jpowsour.2013.12.081

sulphur composites utilizing active carbon, carbon nanotubes [10,11], carbon fibres [12,13], mesoporous/porous carbon [14–18], graphene and modified graphene [19–28] have been proposed. These types of composites have helped to overcome the problems, which focus on enhancing the electrical conductivity of the cathode and suppressing the diffusion of soluble polysulphide intermediates during cycling. Nevertheless, it remains a challenging task to retain a high and stable capacity of sulphur cathodes for more than 100 cycles.

Graphene has been considered as one of the most important conductive carbon matrixes for Li-S batteries. It has many advantages such as very high electrical conductivity, large surface area, and tuneable surface properties, which are beneficial for energy storage devices [3]. It is a two-dimensional electronic conductor exhibiting high chemical stability, excellent mechanical strength and flexibility [19–28]. Graphene oxide (GO), prepared by several different oxidation processes, is probably the most promising way of the synthesis of graphene [29]. A number of studies have been conducted on combination of graphene and sulphur to fabricate Li-S batteries' cathodes and it was found that the batteries' performances are improved. For example, when GO was used as matrix to immobilize sulphur, uniform and thin coating of sulphur on GO sheets has been successfully obtained [20]. Developed Li-S cells using this GO-S composite demonstrate reversible capacity of 850–1400 mA h g^{-1}. In another approach using reduced GO, Zhou et al. [30] used hydrothermally reduced graphene oxide and Wang et al. used thermally expanded graphite oxide to combine with sulphur in cathodes [31]. It is revealed that the oxygen-containing groups on GO have strong binding with polysulphides through S–O bonding, which prevent them from dissolution into the electrolyte [30]. As the result, the GO-S composite cathodes show good specific capacity and stable cyclability over 100 cycles.

Nanofibrillated cellulose (NFC) consists of nano-sized cellulose fibrils that entangle into three-dimensional network with high aspect ratio [32]. The term nanofibrillated cellulose is often named as nanocellulose for simplicity. NFC is known as the biodegradable polymer which is non-toxic to human and environment friendly. We have reported that the combination of amine-functionalized NFC and chemically reduced GO (RGO) resulted in graphene nanocomposite paper with high mechanical properties and excellent electrical conductivity [33]. In this study, we combined the nanocellulose and RGO in a well-controlled manner to make porous and conductive NFC/RGO composite for sulphur deposition. The obtained NFC/RGO/S composite material was used to fabricate positive electrode for Li-S battery. The nanocellulose network acts as a structural frame [34] for the graphene-sulphur composite and prevents the opening of graphene sheets due to volume expansion caused by formation of Li_2S during sulphur reduction.

In this work, we report on the electrochemical behaviour of three different mixtures of graphene/cellulose as a host matrix in Li-S batteries. We demonstrate the effect of the ratio of graphene/cellulose, the role of electrode morphology, and we give possible explanations regarding the capacity fading observed in this system.

2. Experimental part

2.1. Materials

Graphite flake (particle size <200 μm), sulphuric acid (95–98%), hydrochloric acid (36 wt.%), potassium permanganate (99+%), sodium nitrate (99.5%), and hydrazine hydrate were purchased from Sigma–Aldrich Co.; ammonia solution (28%) was obtained from VWR Co., and hydrogen peroxide (30%) was obtained from Merck. Nanofibrillated cellulose (NFC) was received from the UPM Corporation (Finland). The material was produced by mechanical disintegration of bleached birch pulp, which was pre-treated with a Voith refiner prior to fibrillation with an M7115 fluidizer from Microfluidics Corp (Newton, MA, USA) [35]. The suspension has a solid content of 1.37 wt.%. The NFC fibrils in the suspensions are mostly 20–30 nm in diameter and several micrometres in length. The NFC was amine-functionalized according to the previous report [32].

2.2. Method

2.2.1. Preparation of graphene oxide

Graphite was oxidized to produce graphite oxide according to a modified Hummers' method [36]. Natural graphite (10 g) was added in a flask containing 250 mL concentrated sulphuric acid. The flask was immersed in an ice bath. An amount of 5 g sodium nitrate was supplied to the mixture while stirring with a magnetic bar. Subsequently, 30 g of potassium permanganate was slowly added to the flask, and the temperature of the reaction was kept below 20 °C. After being mixed for an hour, the mixture was heated to 35 °C and kept at this condition for 1.5 h. The mixture was then cooled down to room temperature and left over night. Then, 200 mL of deionized (DI) water was added slowly in 0.5 h. Next, 50 mL of hydrogen peroxide was injected to the mixture for 0.5 h. In the next step, 500 mL of DI water was poured into the flask. The mixture was washed with 1.5 L of 5 wt% HCl solution. The mixture was then washed with DI water and dried. The obtained graphite oxide (GO) in this stage was exfoliated in DI water by ultrasonic equipment (solid content 1 g of GO in 400 mL). The sonicated mixture was centrifuged at 4000 rpm for 20 min to remove the precipitate, and the dispersion was graphene oxide. Solid content of exfoliated GO sheets in the dispersion was measured to be around 2 mg mL^{-1}.

2.2.2. Preparation of NFC/RGO composite powder

NFC suspension was added to the GO dispersion while stirring with a magnetic bar. The solid content of GO/NFC was controlled to be 30/70, 50/50, and 70/30 wt/wt. The pH of the mixture was adjusted to around 10 with the ammonia solution. Hydrazine was added to the mixture as the reducing agent for GO to produce reduced graphene oxide (RGO). The amount of hydrazine was 100 μL per 100 mg of solid GO. The mixture was then heated to 95 °C and kept at this condition for 2 h for reaction completion. The mixture was cooled down to room temperature and solidified in liquid nitrogen, after which it was freeze-dried for 72 h to eliminate water, ammonia and excess hydrazine. Samples are denoted in the text as GC37 for 30/70 mixture, GC55 for 50/50 mixture and GC73 for 70/30 mixture.

2.2.3. Preparation of graphene/cellulose-sulphur (GCS) composite

A graphene/cellulose carbon matrix with three different ratios of graphene and cellulose (30:70, 50:50, 70:30) was dispersed in dichloromethane by an ultra-speed rotor for 5 min; next, sulphur dissolved in dichloromethane was added to dispersed graphene/cellulose carbon matrix and sonicated for 5 min, before removing the solvent by using rotor vapour at 40 °C. The obtained mixture was dried at 50 °C overnight and then heated at 155 °C for 6 h in an argon atmosphere to encapsulate sulphur in the graphene/cellulose composite. The content of sulphur was checked via elemental analysis (CHNS) to estimate the amount of sulphur in the composite. All the samples showed 50 wt.% sulphur in the composite. A sample with 30:70 graphene:cellulose was termed GCS37; a sample with 50:50 graphene:cellulose was termed GCS55, and a sample with 70:30 graphene:cellulose was termed GCS73.

Nitrogen adsorption–desorption isotherms were measured at −196 °C using a Tristar 3000 (Micromeritics, Norcross, GA, USA). Before the measurement, the template-free sample was outgassed for 12 h at 105 °C and for 1 h at 150 °C in the degas port of the

instrument. The BET-specific surface area was calculated by using adsorption data in the relative pressure range from 0.05 to 0.16.

2.2.4. Materials characterisation

A field-emission scanning electron microscope (FE SEM Supra 35 VP Carl Zeiss) was used to obtain scanning electron microscope (SEM) images of the materials. JEM-2100 Transmission Electron Microscope was used to obtain the transmission electron microscope (TEM) images of the samples. Raman spectroscopy data of the NFC/RGO samples were obtained with the help of WI Tec alpha 300 instrument.

2.2.5. Electrode preparation and electrochemical characterization

Electrodes from the composite were prepared by making slurry of composite, PVDF and carbon black (Vulcan) in a % weight ratio of 85:7:8. The slurry was then cast on the surface of aluminium foil, using the doctor blade technique. Dried electrodes were used to assemble a coffee bag battery in an argon-filled glove box, where 1 M LiTFSI in sulfolane was used as electrolyte and pure lithium metal was used as anode electrode. The sulphur loading was 2 mg cm^{-2} among the electrodes. Electrodes were separated with a glass wool separator, and the amount of electrolyte used in all experiments was normalized per active mass; it was 60 μL per mg of sulphur. Galvanostatic cycling was performed at room temperature by using a Bio-Logic VMP3 instrument with current density of 167.5 mAg^{-1} in the potential window between 3 V and 1.5 V versus metallic lithium at C/10 rate for the discussed measurements. Columbic efficiency was calculated as a ratio between discharge capacity and charge capacity obtained from previous charging.

3. Results and discussion

The prepared NFC/RGO composites are lightweight materials, which is indicative of their highly open structure, appropriate for the infiltration of sulphur. In our work, we used three samples with different ratios of graphene and cellulose. Sample GC55 (1:1 weight ratio) has been checked with microscopy and representative micrographs are shown in a Fig. 1. The SEM micrograph (Fig. 1a) confirms that the open structure and large graphene flakes can be observed. The presence of graphene flakes and cellulose fibres was better observed by using a TEM microscope (Fig. 1b–d). Interlaced graphene flakes and cellulose nanofibrils formed a three dimensional host matrix with laminar pores (Fig. 1d). The uniform distribution of graphene flakes provided good conditions for sulphur impregnation due to laminar voids. Such microstructures can enable sulphur electrochemical reaction to Li_2S due to the presence of highly conductive graphene. Additionally, the presence of voids provided sufficient space to accommodate volume expansion, which occurs during the sulphur reduction.

In order to quantify surface area, pore volume and pore distribution, we measured nitrogen adsorption isotherms for all three samples. None of samples showed any microporosity, as can be observed in Fig. 2. The shape of adsorption isotherms is close to type III isotherms for which it is characteristic that multilayers of nitrogen are already formed at low pressure. That confirms the presence of large laminar voids without any microporosity. Only sample GC55 showed small deviation from type III with a hysteresis. In all three samples, the average pore size was around 50 nm with slightly uneven pore size distribution. The calculated BET-specific surface area ranged from 28.8 m^2g^{-1} for GC37, 60.0 m^2g^{-1} for GC55 and 41.1 m^2g^{-1} for GC73. Samples exhibit a relative low surface area to be used as host matrix for sulphur impregnation; however, this low surface area was due to the absence of microporosity. Based on the pore size, the BET and the estimated pore volume were restricted to load 50 wt.% of sulphur in all composites. Such loading should enable encapsulation of polysulphides and accommodation of Li_2S.

The thickness and the quality of the graphene along with a signal from cellulose were checked with Raman spectroscopy (Fig. 3). All three samples have a G band at 1585 cm^1, which is indicative of multilayer graphene flakes, since the G-band appears in mono-layer graphene at 1582 cm^{-1} [37,38]. The D peak at 1345 cm^{-1} is derived from disordered structure of the graphene sheets which is caused by the remaining oxygen functionalities and defects by chemical reduction, similar to many reported results related to graphene work [38,39]. All the samples possessed higher intensity of D band, which was most probably due to the presence of irrational ratios of graphene and cellulose or because of more defects at the edges of the graphene layers.

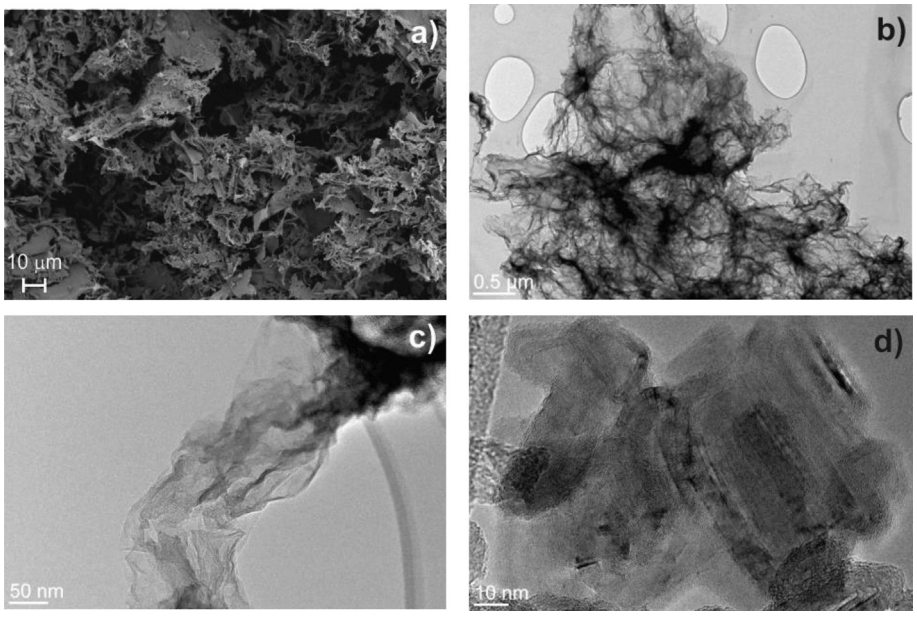

Fig. 1. As prepared graphene/cellulose composite (GC55) a) SEM micrograph b) – d) TEM micrographs.

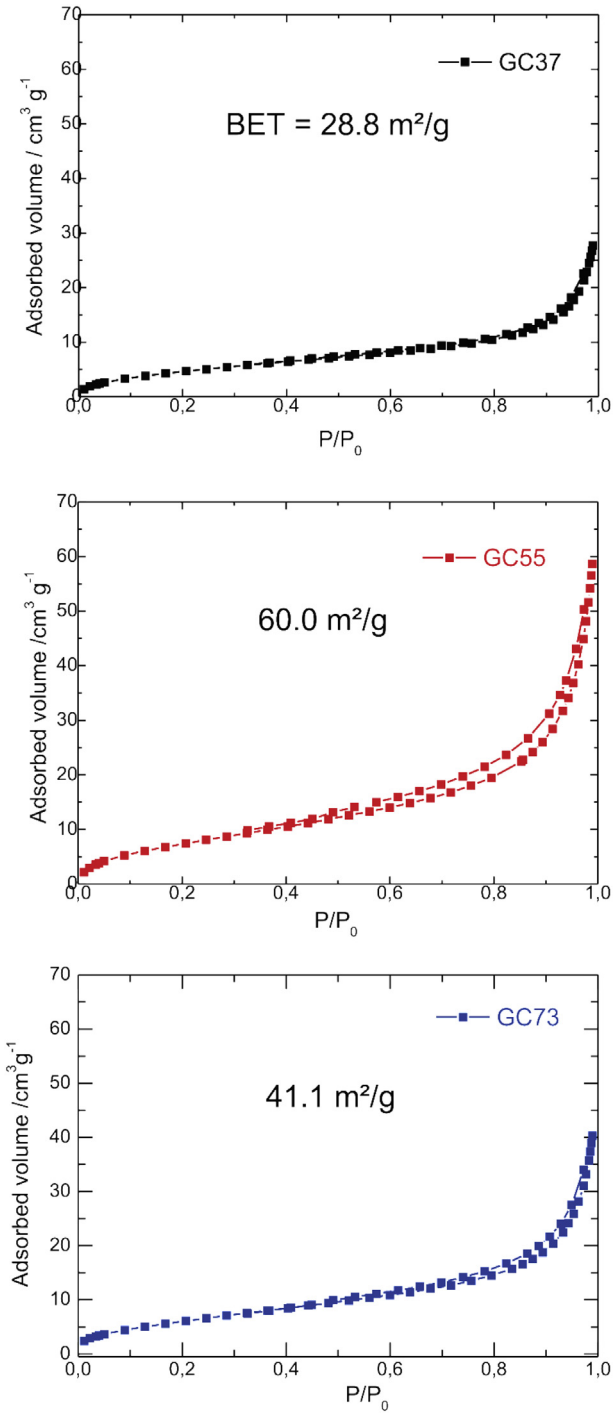

Fig. 2. N2 adsorption isotherms and related BET surface area of graphene/cellulose composites a) GC37 composite, b) GC55 composite and c) GC73 composite.

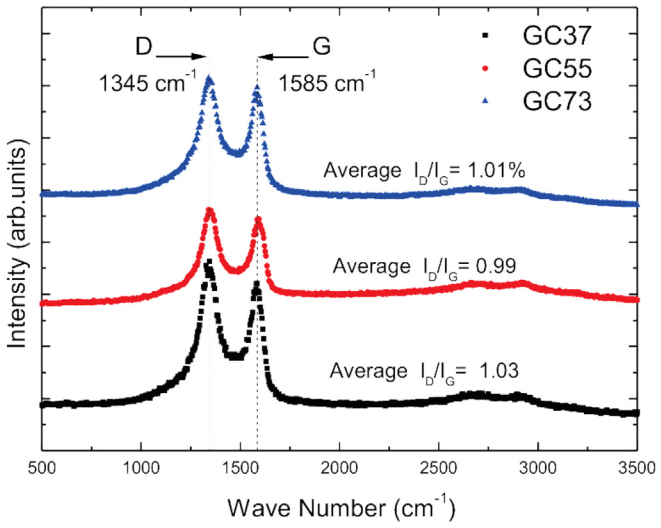

Fig. 3. Raman spectra of graphene/cellulose composites.

Fig. 4 shows the electrochemical cycling performance of NFC/RGO composites. Two sets of electrochemical cycling were performed; in one set, we used non-pressed (as prepared) electrodes, and for the second we used pressed electrodes. The cycling performance of non-pressed and pressed electrodes showed the same trend in the capacity retention: GCS55 presented the highest discharge capacity in both cases, although the difference after pressing was much smaller. A similar trend was observed comparing GCS37 and GCS73. Comparison of the initial cycle performance (first discharge and charge) for all three composites (Fig. 4c–d) showed a higher polarisation of the battery where we used low ratio of graphene in the composite (GCS37). That was more pronounced in the batteries that were not pressed, while in the pressed batteries a difference between polarisation was almost negligible (Fig. 4d). Composites with the higher ratio of graphene showed similar positions of the high and low voltage plateaus. From these set of measurements with un-pressed and with pressed electrodes, we would like to point out two futures. When we used non-pressed electrodes, capacity fading was much faster compared to batteries assembled with pressed electrodes. In our opinion, the reason for such difference is due to the accessibility of the electrolyte within the electrode. As presented in Fig. 1, NFC/RGO composites exhibit high open volume, which can be successfully used for infiltration of sulphur and electrolyte. A larger volume corresponds to higher solubility; with this, there is a higher probability for polysulphide diffusion. In the pressed electrodes, the porosity is closed. That potentially prevented the diffusion of polysulphides; however, with pressing the open volume was closed, which could have led to the isolation of sulphur, or the volume required for the formation of Li_2S was reduced. SEM micrographs of the surface of electrodes from non-pressed (Fig. 5a) and pressed electrodes (Fig. 5b) partially confirm our prediction, since non-pressed electrodes prepared with the sulphur-impregnated GCS55 composite showed very similar morphology as the GC55 composite (Fig. 1a). The morphology of pressed electrodes exhibited partially closed surfaces, which in our opinion blocked the electrochemical conversion of sulphur to lithium sulphide in some parts of the electrode. The morphology of electrodes was preserved after cycling as shown in SEM micrographs in Fig. 5c and d. Nevertheless, the electrochemically active parts were losing active components more slowly and consequently the capacity fading was much less compared to non-pressed electrodes. Nevertheless, such capacity fading is not optimal for the commercial use since the battery lost approximately 23.8% of capacity from the third to 100th cycle. However, this result is in line with most of the recent reports, where similar capacity fading has been observed with more complicated host structures possessing honeycomb structures, closed pore structures or structures with a dual porosity. Further improvement could be possible with an integrated approach in which attention is given to the separator, electrolyte and lithium surface. The second feature observed from galvanostatic cycling experiments was the columbic efficiency. In both sets of experiments, we cannot neglect the additional sporadic process that

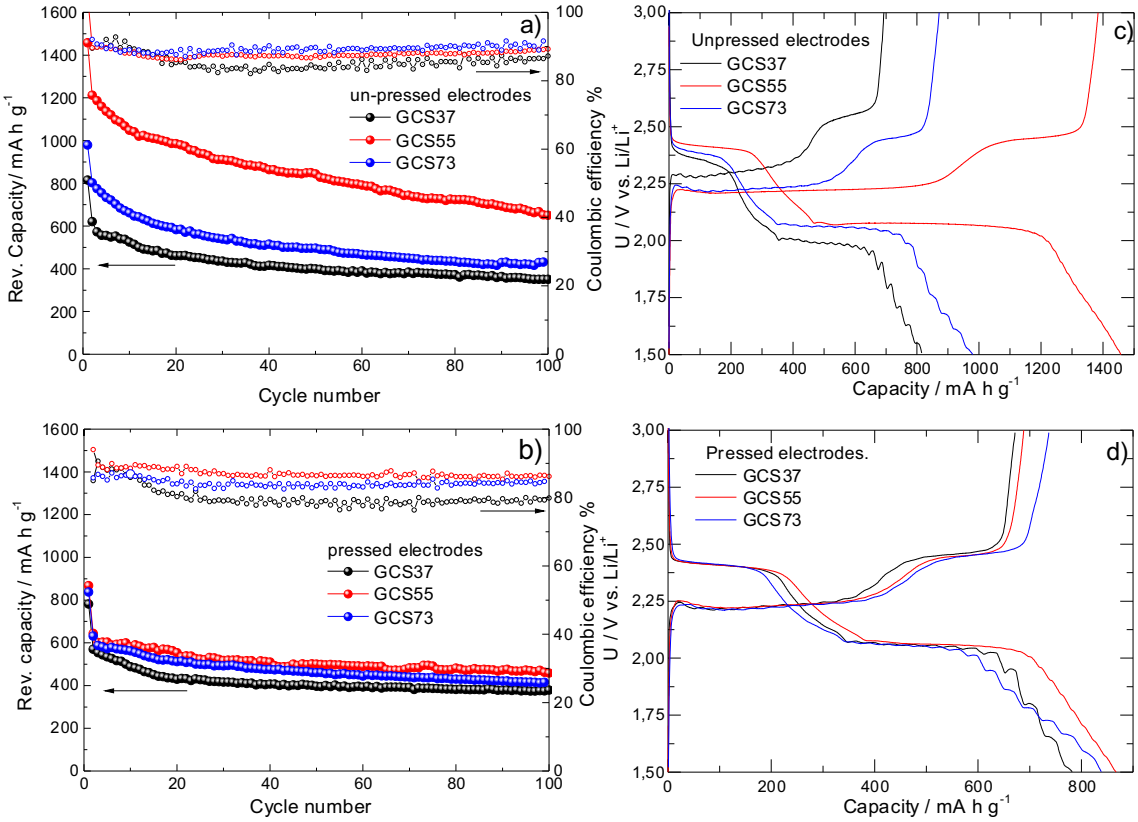

Fig. 4. Discharge capacity (left axis) and columbic efficiency (right axis) of GCS composites over 100 cycles for un-pressed and pressed electrodes (a) and (b) and a first cycle discharge/charge curves for un-pressed and pressed electrodes (c) and (d).

consumes charge during battery charging. The possible explanations are oxidation of the electrolyte or polysulphide shuttle mechanism. The occurrence of the shuttle mechanism was more probable since the capacity drop in the formation cycles was very similar, and it did not depend on the pre-treatment of the electrode (pressed vs. non-pressed). Whatever the graphene/cellulose composite we used and whether it was pressed or not, we observed a capacity drop of approximately 200 $mAhg^{-1}$ from the first to

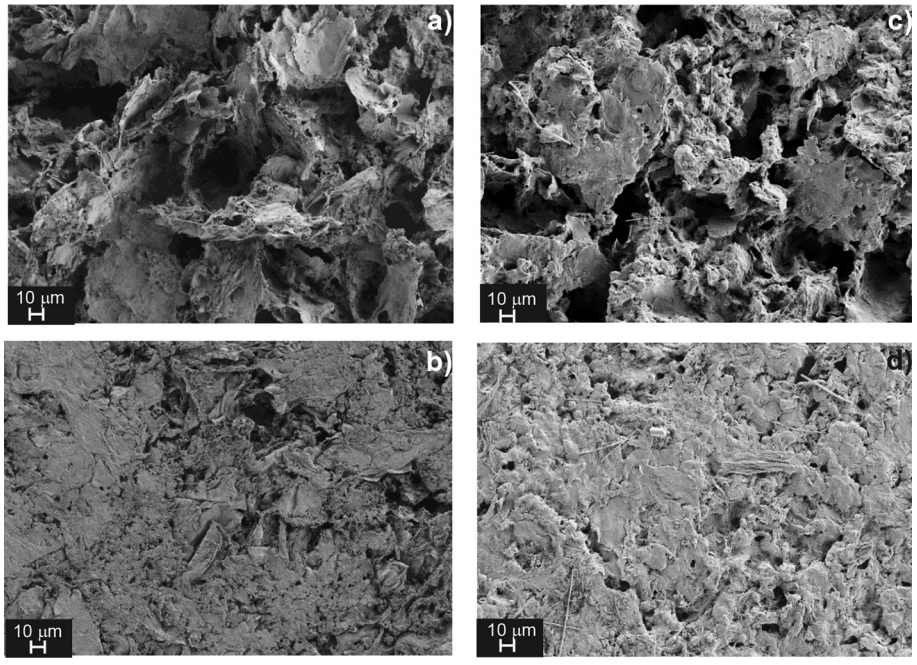

Fig. 5. SEM micrographs of un-pressed and pressed electrodes prepared by using GCS55 composite before cycling (a) and (b) and after cycling (c) and (d).

second discharge. Probably, this capacity drop is due to sulphur present on the surface of the electrode, which can be diffused away from the positive electrode in the first cycle and creates shuttle mechanism in higher cycles. This indicates the necessity of effective separation of sulphur compounds and metallic lithium. Once the sulphur compounds are in the vicinity of the negative electrode (metallic lithium), they can independently create a polysulphide shuttle mechanism to release any of the active component in higher cycles. In our opinion, this explains the slightly lower columbic efficiency in the set of experiments with pressed electrodes.

To verify if the reason for low efficiency was due to electrolyte consumption, we continued with a cycling of GCS55 composite in the pressed electrode. Fig. 6a shows discharge/charge capacities in 200 cycles together with columbic efficiency. The capacity drop from 100th to 200th cycle was an additional 10%, suggesting on the slow loss of active component. More importantly, comparing discharge/charge curves (Fig. 6b), we were not able to detect any considerable increase of the polarisation. This observation can be understood as a process in which the reason for the capacity drop was not due to increase of inner resistance (formation of passive films or/and electrode dry out), but rather due to loss of contacts with reduced product of sulphur.

This work has demonstrated that it is not necessary to have a host structure in the form of complicated porous materials with a designed porosity; in fact, a proper confinement can help to avoid the diffusion of polysulphides. Our work indicates that the absence

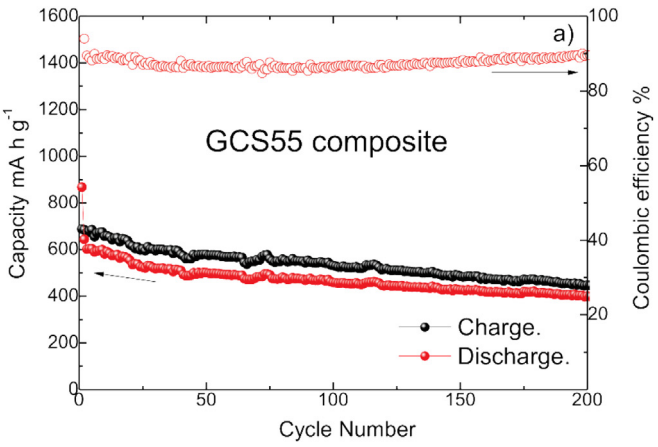

Fig. 6. a) Discharge/charge capacity and columbic efficiency for GCS55 composite and b) electrochemical discharge/charge curves in the selected cycles.

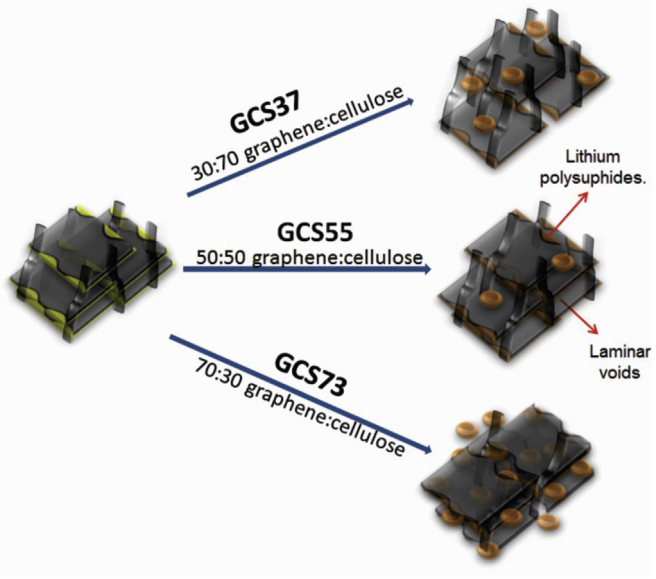

Fig. 7. Proposed model of Li-S battery behaviour with different ratios of graphene and cellulose.

of microporosity still results similar electrochemical characteristics, as attested to by the majority of results in the literature. However, the difference in the electrochemical activity between different sulphur-impregnated graphene cellulose composites indicates the importance of the engineering of host matrix for sulphur impregnation. Based on our work, we can propose the following scenario, which occurred by using graphene/cellulose composites with different ratios between graphene and cellulose (Fig. 7). Less graphene in the composite (sample GC37) corresponded to worse electronic contacts and reduced the number of voids in the composite. In contrast, by reducing cellulose in the composite (sample GC73), graphene flakes cannot be separated and consequently there are not enough voids for the encapsulation of sulphur and polysulphides. From these preliminary experiments, it seems that mixture of 1:1 between graphene and cellulose (sample GC55) forms the microstructure, which can restrain polysulphides and accommodate volume expansion during the reduction process. We propose that with further engineering and modification of the surfaces, more stable capacity retention can be achieved.

4. Conclusions

Composites of graphene and cellulose were successfully used as a host matrix for sulphur impregnation and tested in Li-S batteries. Prepared mixtures between graphene and cellulose exhibited relative low surface area; however, laminar pore structure enabled 50 wt.% of sulphur impregnation. The best electrochemical behaviour was obtained with a graphene/cellulose ratio of 1:1, with capacity over 1200 $mAhg^{-1}$ in the formation cycles accompanied with quick capacity fading. More stable capacity fading has been obtained with the pressed electrodes, and in first 200 cycles about one third of capacity was lost without any indication of increase of polarisation within the battery. This work indicates that simple host matrixes can be successfully utilized for sulphur impregnation.

Acknowledgements

This research has received funding from the Slovenian Research Agency research programme P2-0148 and a research project J2-

5469. RD acknowledges a support from the European Union Seventh Framework Programme under grant agreement No. 314515 (EUROLIS). UPM-Kymmene Corporation (Finland) is acknowledged for delivering UPM Fibril Cellulose™ raw material. Nikolaos Pahimanolis is thanked for the amine functionalization of NFC.

References

[1] P.G. Bruce, L.J. Hardwick, K.M. Abraham, MRS Bull. 36 (2011) 506–512.
[2] A. Manthiram, Y. Fu, Y.-S. Su, Acc. Chem. Res. 46 (2013) 1125–1134.
[3] S. Evers, L.F. Nazar, Acc. Chem. Res. 46 (2013) 1135–1143.
[4] J. Wang, S.Y. Chew, Z.W. Zhao, S. Ashraf, D. Wexler, J. Chen, S.H. Ng, S.L. Chou, H.K. Liu, Carbon 46 (2008) 229–235.
[5] Y.-S. Su, A. Manthiram, Nat. Commun. (2012), http://dx.doi.org/10.1038/ncomms2163.
[6] Y.V. Mikhaylik, J.R. Akridge, J. Electrochem. Soc. 151 (2004) A1969–A1976.
[7] L. Yin, J. Wang, F. Lin, J. Yang, Y. Nuli, Energy Environ. Sci. 5 (2012) 6966–6972.
[8] C. Zhang, H.B. Wu, C. Yuan, Z. Guo, X.W. Lou, Angew. Chem. Int. Ed. 51 (2012) 9592–9595.
[9] Y.-S. Su, A. Manthiram, Chem. Commun. 48 (2012) 8817–8819.
[10] S. Dörfler, M. Hagen, H. Althues, J. Tübke, S. Kaskel, M.J. Hoffmann, Chem. Commun. 48 (2012) 4097–4099.
[11] J. Guo, Y. Xu, C. Wang, Nano Lett. 11 (2011) 4288–4294.
[12] L. Ji, M. Rao, S. Aloni, L. Wang, E.J. Cairns, Y. Zhang, Energy Environ. Sci. 4 (2011) 5053–5059.
[13] R. Elazari, G. Salitra, A. Garsuch, A. Panchenko, D. Aurbach, Adv. Mater. 23 (2011) 5641–5644.
[14] C. Liang, N.J. Dudney, J.Y. Howe, Chem. Mater. 21 (2009) 4724–4730.
[15] X. Ji, K.T. Lee, L.F. Nazar, Nat. Mater. 8 (2009) 500–506.
[16] G. He, X. Ji, L.F. Nazar, Energy Environ. Sci. 4 (2011) 2878–2883.
[17] D. Li, F. Han, S. Wang, F. Cheng, Q. Sun, W.-C. Li, ACS Appl. Mater. Interfaces 5 (2013) 2208–2213.
[18] N. Jayaprakash, J. Shen, S.S. Moganty, A. Corona, L.A. Archer, Angew. Chem. Int. Ed. 50 (2011) 5904–5908.
[19] H. Wang, Y. Yang, Y. Liang, J.T. Robinson, Y. Li, A. Jackson, Y. Cui, H. Dai, Nano Lett. 11 (2011) 2644–2647.
[20] L. Ji, M. Rao, H. Zheng, L. Zhang, Y. Li, W. Duan, J. Guo, E.J. Cairns, Y. Zhang, J. Am. Chem. Soc. 133 (2011) 18522–18525.
[21] S. Evers, L.F. Nazar, Chem. Commun. 48 (2012) 1233–1235.
[22] F.-F. Zhang, X.-B. Zhang, Y.-H. Dong, L.-M. Wang, Mater. Chem. 22 (2012) 11452–11454.
[23] T. Lin, Y. Tang, Y. Wang, H. Bi, Z. Liu, F. Huang, X. Xiec, M. Jiang, Energy Environ. Sci. 6 (2013) 1283–1290.
[24] B. Ding, C. Yuan, L. Shen, G. Xu, P. Nie, Q. Laia, X. Zhang, J. Mater. Chem. A 1 (2013) 1096–1101.
[25] M. Xiao, M. Huang, S. Zeng, D. Han, S. Wang, L. Sunb, Y. Meng, RSC Adv. 3 (2013) 4914–4916.
[26] J. Jin, Z. Wen, G. Ma, Y. Lu, Y. Cui, M. Wu, X. Liang, X. Wu, RSC Adv. 3 (2013) 2558–2560.
[27] N. Li, M. Zheng, H. Lu, Z. Hu, C. Shen, X. Chang, G. Ji, J. Cao, Y. Sh, Chem. Commun. 4 (2012) 4106–4108.
[28] Y. Cao, X. Li, I.A. Aksay, J. Lemmon, Z. Nie, Z. Yang, J. Liu, Phys. Chem. Chem. Phys. 13 (2011) 7660–7665.
[29] D.R. Dreyer, S. Park, C.W. Bielawski, et al., Chem. Soc. Rev. 39 (2010) 228–240.
[30] G. Zhou, L.-C. Yin, D.-W. Wang, et al., ACS Nano 7 (2013) 5367–5375.
[31] Y.-X. Wang, L. Huang, L.-C. Sun, et al., J. Mater. Chem. 22 (2012) 4744–4750.
[32] N.D. Luong, J.T. Korhonen, A.J. Soininen, et al., Eur. Polym. J. 49 (2013) 335–344.
[33] N.D. Luong, N. Pahimanolis, U. Hippi, et al., J. Mater. Chem. 21 (2011) 13991–13998.
[34] Z. Shi, G.O. Phillips, G. Yang, Nanoscale 5 (2013) 3194–3201.
[35] M. Pääkkö, M. Ankerfors, A. Nykänen, S. Ahola, M. Östergerg, J. Ruokolainen, J. Laine, P.T. Larsson, O. Ikkala, T. Lindström, Biol. Macromol. 8 (2007) 1934–1941.
[36] J.W. Hummers, R.E. Offeman, J. Am. Chem. Soc. 80 (1958) 1339.
[37] L.M. Malard, M.A. Pimenta, G. Dresselhaus, M.S. Dresselhaus, Phys. Rep. 473 (2009) 51–87.
[38] A.C. Ferrari, J.C. Meyer, V. Scardaci, C. Casiraghi, M. Lazzeri, F. Mauri, S. Piscanec, D. Jiang, K.S. Novoselov, S. Roth, A.K. Geim, PRL 97 (2006) 187401–187404.
[39] L.S. Panchakarla, K.S. Subrahmanyam, S.K. Saha, A. Govindaraj, H. Krishnamurthy, U.V. Waghmare, C.N.R. Rao, Adv. Mater. 21 (2009) 4726–4730.